J. Iran. Chem. Soc., Vol. 8, No. Suppl., February 2011, pp. S110-S118.

JOURNAL OF THE
Iranian
Chemical Society

DFT Study of CH_4 Adsorption on the (5,0), (4,4), (5,5) and (6,6) Single-Walled Carbon Nanotubes. Calculated Binding Energies, NMR and NQR Parameters

B.B. Shirvani[a], M.B. Shirvani[b], J. Beheshtian[a] and N.L. Hadipour[a,*]

[a]*Department of Chemistry, Tarbiat Modares University, P.O. Box: 14115-175, Tehran, Iran*

[b]*Department of Mathematics, Payame Noor University, Borujen, Iran*

(Received 24 January 2010, Accepted 29 July 2010)

Behavior of a single CH_4 molecule adsorbed on external surface of H-capped (4,4) (5,5), (6,6) and (5,0) single-walled carbon nanotubes (SWCNTs) is studied *via* B97D hybrid density functional and 6-31G* basis set. Binding energies clearly exhibit adsorption dependence on tube diameter. ^{13}C and ^{1}H chemical shielding tensors are calculated at the B971 level using GIAO method. The ^{1}H and $^{13}C(CH_4)$ NMR results reveal that chemical shielding due to CH_4 molecule adsorption are also dependent upon the nanotube electronic structure, and radius. ^{2}H nuclear quadrupole coupling constants, C_Q, and asymmetry parameter, η, reveal the remarkable effect of CH_4 adsorption on electronic structure of the SWCNTs.

Keywords: Single-walled carbon nanotube, Binding energy, Chemical shielding, NMR

INTRODUCTION

A SWNT can be viewed as a rolled graphene sheet and is classified by a vector connecting the two points that meet upon rolling. There are three classes of nanotube: armchair, zigzag, and chiral. These are labeled by (*n,m*), (*n,0*), and (*n,m*), respectively. One of the most striking features of SWNTs is that their electronic structures depend on the chirality and diameter [1]. SWNTs are (1) metals when $n = m$, (2) narrow-gap semimetals when n-m is a multiple of three, and (3) moderate-gap semiconductors otherwise, where (*n*,*m*) is the chiral index [1,2]. The adsorption of gases on and inside carbon nanotubes at low temperatures has been extensively studied. Hydrogen is of particular interest for energy applications. Additionally, the physisorption of Xe [3,4] and CF_4 [5] has recently been examined. The adsorption of gases, particularly CH_4, C_2H_2, C_2H_4, CH_3OH [6]; CO and NO [7]; and NH_3 [8] on a similar substrate, C_{60}, has also been studied. For CH_4, C_2H_2, C_2H_4, CO and NO, the adsorption was shown to be caused by dispersion forces (*i.e.*, physisorption). Because of the weakness of the interaction, these gases would adsorb only below room temperature.

A variety of techniques such as scanning tunneling microscopy (STM) [9], optical adsorption [10], fluorescence spectroscopy [11] and Raman scattering [12] have already been applied to the characterization of SWNT samples. Unfortunately, these techniques even in combination do not provide a full characterization [13]. Thus, the development of alternative techniques is desired. ^{13}C nuclear magnetic resonance (NMR) spectroscopy is one possible choice. Nuclear experimental techniques such as nuclear magnetic resonance (NMR) [14] and nuclear quadrupolar resonance (NQR) [15] are widely used to study the geometry and electronic structure of molecules and solids. NMR measures the local magnetic fields on a nucleus, generated by response of electrons to an external uniform magnetic field. In order to

*Corresponding author. E-mail: hadipour@modares.ac.ir

form a non-degenerated energy spectrum, both NMR and NQR techniques are applied to produce high external magnetic fields and some kind of internal interaction; *i.e.*, the spin-spin interaction in NMR [16-18] and the interaction of quadrupole moment with electron field gradient (EFG) in NQR [19-21]. Both of the interactions are determined by internal properties of crystal. However, the field has recently started to bloom, and an increasing amount of experimental and theoretical data is becoming available.

Most computational solid-state and quantum-chemical studies of SWNTs have so far focused on geometric and electronic structure as well as mechanical properties. It is important to study electric and magnetic response properties as well, since they are the observables of some of the most powerful and frequently applied spectroscopic methods used for characterizing molecules. Among those, NMR is of high practical importance. Previous theoretical work proposed that separation of metallic from semiconducting SWNTs may be possible using high resolution ^{13}C NMR, based on a predicted 11 ppm difference in their chemical shifts [22,23]. Solid-state ^{13}C NMR has been applied to characterize nanotube carbons in the functionalized SWCNT samples [24,25]. The signals corresponding to sp^2 carbons of nanotube are generally broad, centered around 120-130 ppm, and similar to those of unfunctionalized SWNTs [26-29].

In this article, DFT calculations were used to study the adsorption of CH_4 on metallic armchair (4,4), (5,5), (6,6) and semi metallic zigzag (5,0), carbon nanotubes. CH_4 effects on ^{13}C and ^{1}H NMR chemical shielding tensors, and difference in nuclear quadrupole resonance parameters, NQR, for ^{2}H nuclei are calculated to obtain useful information about the nature of interactions.

COMPUTATIONAL DETAILS

Full geometry optimizations are performed for the (5,0), (4,4), (5,5) and (6,6) pristine and functionalized SWCNTs using *Gamess* and *Gaussian* suite of programs [30]. Geometry optimizations are carried out using B97D hybrid density functional and 6-31G* basis set [31]. The B97D functional was chosen because, among the presently available functionals, it give a better description of dispersion interactions, and hence, of the physical adsorption. The starting geometries are generated using *TubeGen* tool [32] based on a hexagonal unit cell. Optimized diameters are 4.10 Å for zigzag and 5.69, 7.03, 8.44 Å for armchair nanotubes, respectively. Length of nanotubes are 13.8 Å and 10.44, 10.46, 10.47 Å, respectively, with an average C-C bond length of 1.43 Å. The adsorption energy is defined by E_{ads} = E (adsorbate and CNT) - E(CNT) - E(adsorbate). Application of localized basis sets largely reduces the amount of computational work required while considering large vacuum regions in the unit cell. The bottom dangling bonds are saturated by hydrogen atoms. Chemical shielding tensors are computed for the pristine and SWCNT-molecule systems using Slater-type gauge-including atomic orbital (GIAO) by B971 hybrid density functional and 6-31G* basis set [33].

The interaction between nuclear electric quadrupole moment and EFG at quadrupole nucleus is described with Hamiltonian:

$$\hat{H} = \frac{e^2 Q V_{zz}}{4I(2I-1)}[(3\hat{I}_z^2 - \hat{I}^2) + \eta_Q(\hat{I}_x^2 - I_y^2)]$$

Here eQ is the nuclear electric quadrupole moment, I is the nuclear spin, and V_{zz} is the largest component of EFG tensor. The principal components of the EFG tensor, V_{ii}, are computed in atomic unit (1 au = 9.717365 × 10^{21} $V\,m^{-2}$), with $|V_{zz}| \geq V_{yy} \geq |V_{xx}|$ and $V_{xx} + V_{yy} + V_{zz} = 0$. These diagonal elements relate to each other by the asymmetry parameter; $\eta = |V_{yy} - V_{xx}|/|V_{zz}|$, $0 \leq \eta \leq 1$, that measures the deviation of EFG tensor from axial symmetry. The computed V_{zz} component of EFG tensor is used to obtain nuclear quadrupole coupling constant from the equation; $C_Q = e^2QV_{zz}/h$ [34], where standard values of $eQ(^2H)$ reported by Pyykkö are employed [35]. EFG calculations at hydrogen nuclei are determined using B971/6-31G* level of theory.

RESULTS AND DISCUSSION

Interaction of Methane with SWCNTs

Interaction of (5,0) zigzag and (4,4), (5,5), (6,6) armchair SWCNTs with a single CH_4 molecule is considered. To find adsorption behavior of CH_4 on SWCNTs, one methane molecule is moved toward the hollow or bridge site of the tube wall, and equilibrium distance of molecule tube are then

found, Fig. 1. Results for binding energies, equilibrium distance and dipole moments of zigzag and armchair tubes with different diameters are presented in Table 1. Calculated adsorption energies tube-CH_4 for (5,0), (4,4), (5,5) and (6,6) are negative. These results are in agreement with previous results [36]. In general, CH_4 molecules are weakly bound to the nanotubes and the tube-molecules interactions can be identified as physisorption. Binding energy is calculated to be -3.22 kcal mol^{-1} for zigzag (5,0) SWCNT. Effect of the tube diameter on stability of the tube-molecules is interesting. For armchair CNTs, Stability of tube-CH_4 decreases as their diameter increases. These results are in agreement with previous results indicating that gaseous molecules binding energy decreases as the diameter of (*n*,*0*) and (*n*,*n*) CNTs increases [37,38]. Results for armchair tubes reveal that *R* is magnified while moving from a small diameter (4,4) SWCNT (*d* = 5.70 Å) to a larger diameter (6,6) tube (*d* = 8.44 Å).

The calculated bond lengths for (5,5) and (6,6) SWCNTs are 3.38 and 3.39 Å, respectively. These values are close to the corresponding those for other armchair SWCNTs [37-39]. When CH_4 molecule is adsorbed on the CNT, dipole moment of the entire system is significantly increased by a factor of about 0.20-0.25 with respect to the vacuum values. This effect can be understood by polarization of the conducting electrons due to physisorption. However, due to different CH_4 configurations on the surface of nanotubes, no regular pattern is detected for magnitude of their dipole moment (Table 1).

^{13}C NMR Chemical Shifts

Previously, it has been indicated that for H-capped fragments, the calculated ^{13}C chemical shielding values are smaller at the ends of tube, compared to the center, if the carbon is directly bound to hydrogen; otherwise, it is larger [39]. To assess the dependence of NMR results on carbon atom position, ^{13}C chemical shielding values of armchair and zigzag tubes are examined. Three different parts of tube axis,

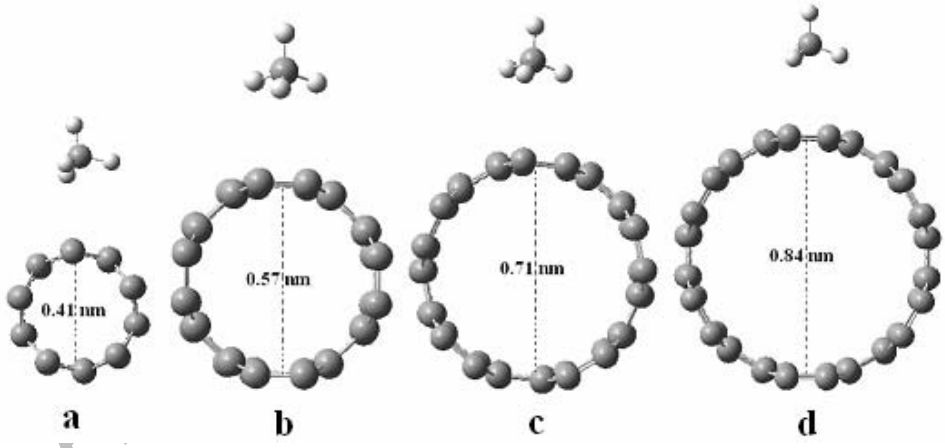

Fig. 1. Equilibrium geometries and pictorial view of the adsorption sites of CH_4-SWCNTs structures: a) (5,0), b) (4,4), c) (5,5) and d) (6,6) CNTs.

Table 1. Calculated Adsorption Energies E_b (kcal mol^{-1}), Equilibrium Tube-Molecule Distance[b] R (Å), and Dipole Moment[a] of the CH_4 Adsorbed on Zigzag (5,0) and Armchair (*n*,*n*), n = 4, 5, 6 Nanotubes

Parameter	(5,0) + CH_4	(4,4) + CH_4	(5,5) + CH_4	(6,6) + CH_4
E_b	-3.22	-3.49	-3.40	-3.29
R	3.40	3.38	3.38	3.39
Dipole moment	0.25	0.20	0.21	0.21

[a]Calculated dipole moment of single CH_4 is 0.00 Debye. [b]CC equilibrium distance.

(two ends and middle parts) are considered (Fig. 2).

Isotropic chemical shielding. Table 2 exhibits the calculated ^{13}C isotropic chemical shielding tensors for various CNTs. CH_4 molecule adsorption on external surface of CNTs has a remarkable influence on ^{13}C NMR tensors, which is in complete accordance with the facts mentioned above. Interesting trends are evidenced: For (5,0) and (4,4) CNTs, the isotropy of ^{13}C shielding tensor are larger at the ends compared to the center (Fig. 2). It can be also seen from Fig. 2 that the isotropy of ^{13}C chemical shielding decreased at the ends compared to the center for armchair tubes with increase of the tube diameter. The shifts are clearly sensitive to the nanotube radius. DFT study of ^{13}C chemical shielding tensors on small-to-medium-diameter infinite SWCNTs reveal a roughly inversely proportional relationship between chemical shielding and tube diameter [40]. It may be noted that ^{13}C chemical shielding tensor at the carbon sites depends remarkably on the tube size and nature of frontier orbitals [41].

According to GIAO calculations performed after adsorption of CH_4 molecule on (5,0) CNT, the isotropy value of the ^{13}C NMR shielding tensor decreases, approximately by 0.63, 0.25, 1.04, ppm, at the C1,C2,C3, (carbon atoms located near CH_4 molecule) sites (Table 2). These shifts are much smaller than those calculated for N-H functionalized finite (11,0), (13,0) and (14,0) CNTs (*ca*., 44 ppm) [42]. As for the armchair (6,6) CNT, the ^{13}C chemical shielding isotropy values are slightly deshielded for all carbon atoms after CH_4 adsorption. In case of (4,4) CNT, the isotropy value of the ^{13}C NMR shielding tensors of interacted carbon atoms are slightly increases the C1,C2, sites as a result of CH_4 adsorption. Comparing pristine (5,5) and tube-molecule, it becomes clear that the C1 and C2 atoms included in CH_4 adsorption are slightly deshielded. The results are consistent with the weak interaction between the tube and CH_4 molecule. The discrepancy between the ^{13}C chemical shielding tensor variation for the zigzag and armchair nanotubes can be attributed to the different nature of the frontier orbitals.

However, it is obvious that there is a large effect of the HOMO on the energies of the HOMO-1 *etc*. which will have an influence on the ^{13}C chemical shieldings (the expression for the paramagnetic shielding tensor contains $(\Delta E_{VO})^{-1}$, the inverse of the energy differences between virtual and occupied orbitals).

Anisotropic chemical shielding. Interesting trends are evidenced: For (5,0), (4,4), (5,5) and (6,6) CNTs, the anisotropy of ^{13}C shielding tensor are smaller at the ends compared to the center (Fig. 2). Table 3 is shown the calculated ^{13}C anisotropic chemical shielding tensors for various CNTs. According to GIAO calculations performed after adsorption of CH_4 molecule on (5,0) CNT, the anisotropy value of the ^{13}C NMR shielding tensor increases for C1 (2.51 ppm), C3 (3.73 ppm), and decreases 0.42 ppm for C2, sites. For the armchair (4,4), (5,5) and (6,6) CNTs, the ^{13}C NMR chemical shielding anisotropy values of interacted carbon atoms are slightly increased after CH_4 adsorption (Table 3). In case of (6,6) CNT, ^{13}C NMR tensors of interacted carbon atoms are also modified as a result of CH_4 adsorption.

Chemical shielding ^{1}H and ^{13}C methane. The ^{13}C and ^{1}H chemical shielding tensors (isotropy and anisotropy) of adsorbed CH_4 molecule on external surface of zigzag (5,0) and armchair (4,4), (5,5), (6,6) CNTs are shown in Table 4. Results indicate that the ^{13}C and ^{1}H NMR chemical shielding are also dependent upon the nanotube electronic structure, and radius. More especially, the ^{13}C NMR isotropy and anisotropy values increase from CH_4 to CH_4-tube. The ^{1}H NMR isotropy value except for (5,0) increased for armchair tubes from CH_4 to CH_4-tubes. However, small differences are detected in proton NMR calculations of the nanotubes. This is mainly due to the limited interaction of hydrogen atoms with nanotubes.

^{2}H NQR Parameters

Due to the physisorption, NQR parameters of hydrogen atoms are also altered. Table 5 indicates the calculated NQR parameters (C_Q, and η) at the hydrogen positions for various SWCNTs. A quick look at the results reveals that the C_Q, and η values for ^{2}H sites are modified by CH_4 adsorption. More especially, the C_Q (^{2}H) parameter decreased at the H_1, H_4 and increased at the H_2,H_3 sites from single CH_4 molecule to CH_4-tube. The asymmetry parameter η (^{2}H) parameter increased from single CH_4 molecule to CH_4-tube. The asymmetry parameter increases (by 0.0003-0.007 units) as result of CH_4-tube interaction. In assessing the significance of C_Q (^{2}H) and η (^{2}H) values, one must keep in mind that electronic contribution to the EFG at hydrogen sites arises almost entirely from mean carbon atoms other than the hydrogen, since near spherical

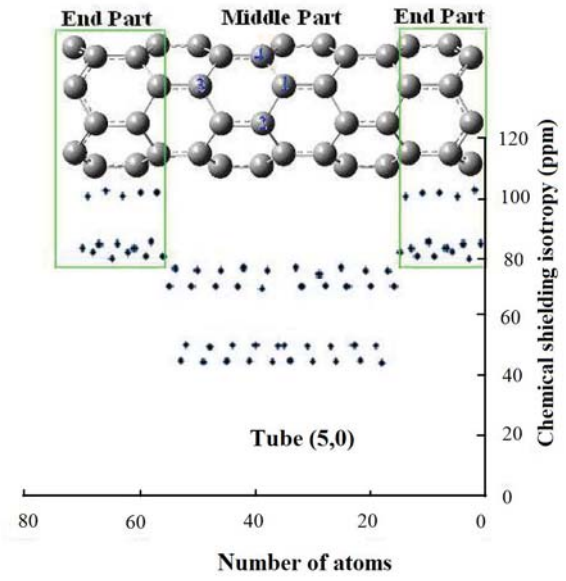
End Part
Middle Part
End Part
Tube (5,0)
Chemical shielding isotropy (ppm)
Number of atoms

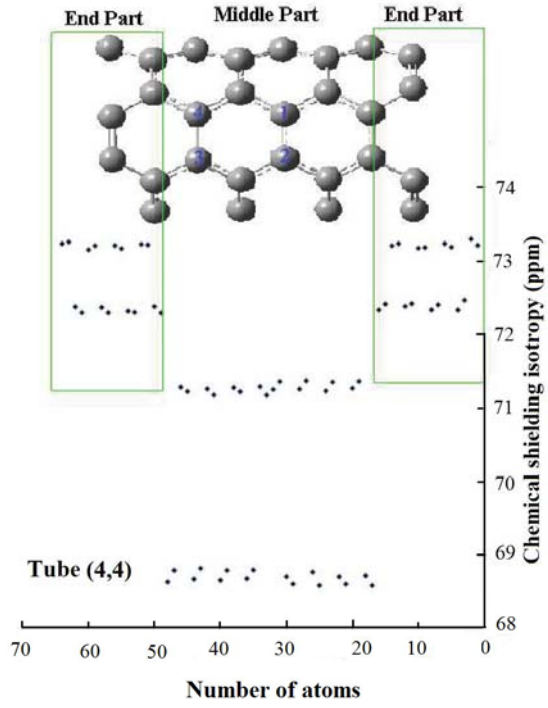
End Part
Middle Part
End Part
Tube (4,4)
Chemical shielding isotropy (ppm)
Number of atoms

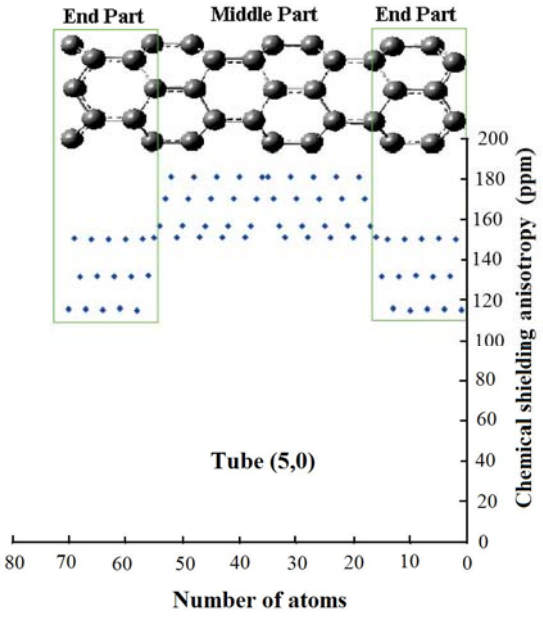
End Part
Middle Part
End Part
Tube (5,0)
Chemical shielding anisotropy (ppm)
Number of atoms

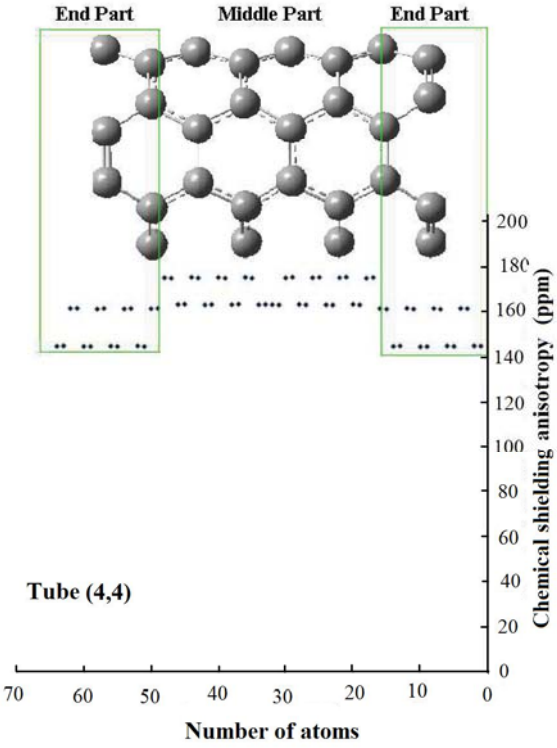
End Part
Middle Part
End Part
Tube (4,4)
Chemical shielding anisotropy (ppm)
Number of atoms

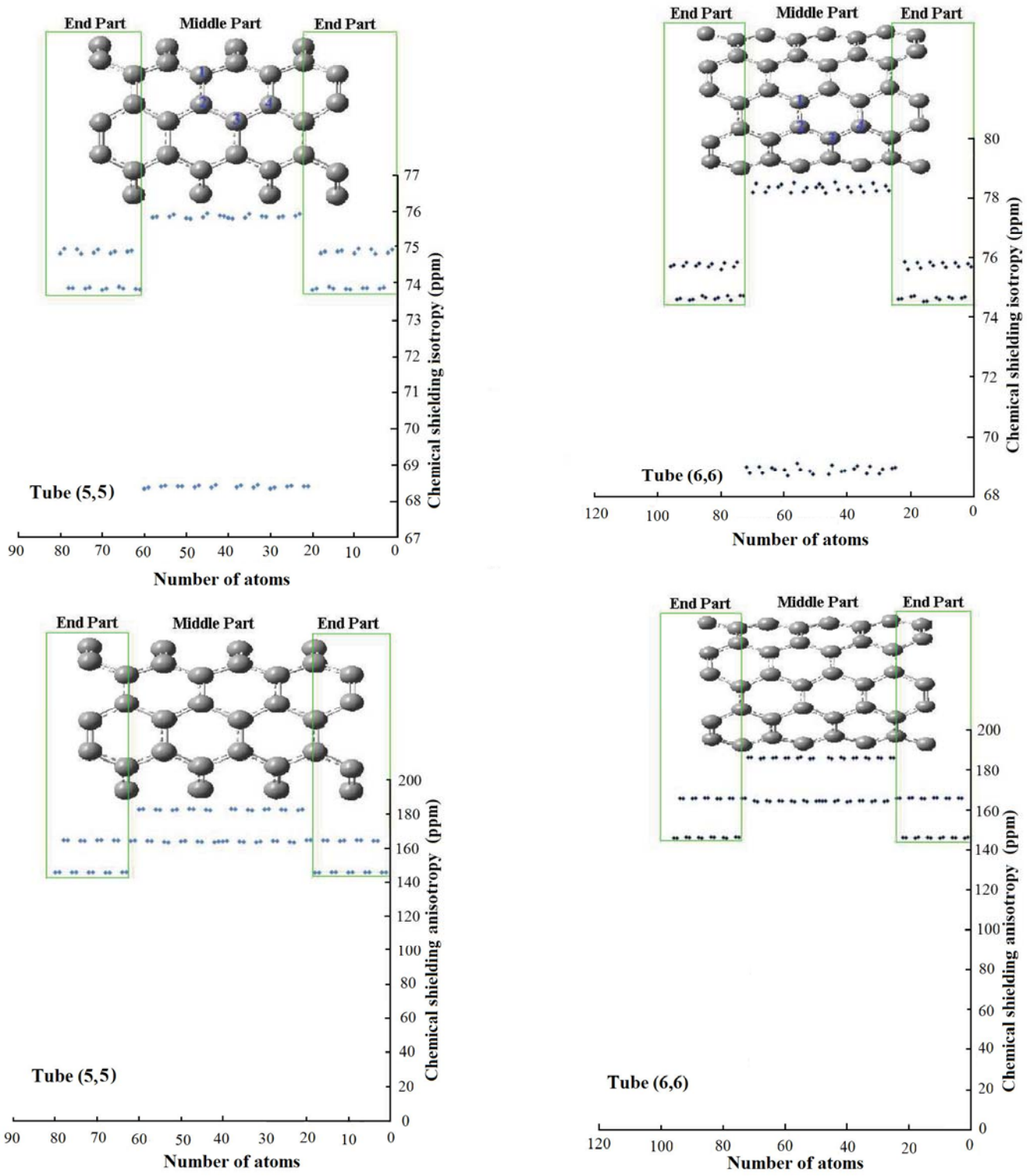

Fig. 2. ^{13}C chemical shielding isotropy and anisotropy values *vs*. carbon atoms number. (5,0), (4,4), (5,5) and (6,6) CNTs.

Table 2. Calculated ^{13}C Chemical Shielding Isotropy Values (in ppm) for SWCNTs

Species	C_1	C_2	C_3	C_4
Tube (5,0)	45.28	45.31	70.42	45.28
Tube (5,0) + CH_4	44.65	45.06	69.38	45.35
Tube (4,4)	68.61	68.79	71.18	71.26
Tube (4,4) + CH_4	68.89	68.88	70.73	70.71
Tube (5,5)	75.87	75.85	68.37	75.81
Tube (5,5) + CH_4	75.79	74.71	68.46	75.87
Tube (6,6)	78.27	78.52	69.12	78.21
Tube (6,6) + CH_4	77.41	77.50	68.85	78.21

Table 3. Calculated ^{13}C Chemical Shielding Anisotropy Values (in ppm) for SWCNTs

Species	C_1	C_2	C_3	C_4
Tube (5,0)	170.26	170.22	151.45	170.38
Tube (5,0) + CH_4	172.77	170.22	155.18	169.96
Tube (4,4)	175.52	175.35	163.31	163.12
Tube (4,4) + CH_4	175.83	175.82	166.62	166.66
Tube (5,5)	164.26	164.38	183.07	164.33
Tube (5,5) + CH_4	166.06	168.55	183.38	164.99
Tube (6,6)	164.76	164.37	186.05	164.63
Tube (6,6) + CH_4	168.78	168.52	187.24	165.23

Table 4. Calculated ^{13}C and ^{1}H Chemical Shielding Isotropy (Anisotropy) Values (in ppm) a Single CH_4 Molecule and for CH_4-SWCNTs

Species	^{13}C	^{1}H	^{1}H	^{1}H	^{1}H
Tube (5,0) + CH_4	191.82(5.83)	31.78(11.76)	31.52(4.04)	31.36(8.23)	31.10(10.65)
Tube (4,4) + CH_4	192.71(12.44)	33.10(8.21)	33.04(8.07)	32.91(13.09)	32.76(15.03)
Tube (5,5) + CH_4	192.29(13.85)	33.41(10.34)	33.25(9.03)	33.09(13.04)	32.93(15.94)
Tube (6,6) + CH_4	193.15(13.58)	33.87(10.55)	33.56(10.47)	33.51(14.10)	33.20(16.76)
Single CH_4	193.16(0.00)	31.70(8.57)	31.70(8.57)	31.70(8.57)	31.70(8.57)

Table 5. Calculated C_Q and η Parameters for SWCNTs and Single CH_4 Molecule[a,b]

Species	$^2H_1$	$^2H_2$	$^2H_3$	$^2H_4$
(5,0) + CH_4	236.13(0.007)	238.44(0.003)	238.28(0.002)	237.74(0.002)
(4,4) + CH_4	237.36(0.006)	238.14(0.002)	238.12(0.002)	237.36(0.0003)
(5,5) + CH_4	237.61(0.004)	238.18(0.002)	238.13(0.002)	237.64(0.0003)
(6,6) + CH_4	237.73(0.005)	238.49(0.003)	238.09(0.003)	237.64(0.0006)
Single CH_4	237.78(0.000)	237.78(0.000)	237.78(0.000)	237.78(0.000)

[a]Calculated C_Q values in kHz for ^2H nuclei. [b]The first value in each cell represents C_Q value, while value within parenthesis indicates η value.

electronic cloud around these nuclei has no contribution. As the CH_4-tube interaction sets in, the electron distribution around the hydrogen nucleus becomes less polarized in the direction of carbon atom and makes a significant reduction in magnitude of all the three individual EFG components.

CONCLUSIONS

Theoretical calculations are performed to characterize the behavior of CH_4 molecule adsorption on external surface of zigzag (5,0), and armchair (4,4), (5,5), (6,6) SWCNTs. Results indicate that as the diameter of armchair tubes increases, the binding energy of CH_4 molecule decreases. According to GIAO calculations, performed after CH_4 adsorption on (5,0) CNT, isotropy value of ^{13}C NMR shielding tensors decreases, approximately by 0.63, 0.25, 1.04, ppm, at the C1,C2,C3, sites whereas the anisotropy value of the ^{13}C NMR shielding tensor increases for C1(2.51 ppm), C3(3.73 ppm), and decreases 0.42 ppm for C2, sites, respectively. In addition, for (4,4), (5,5), (6,6) tubes are slightly increased anisotropy value of the ^{13}C NMR shielding tensor after CH_4 adsorption. The ^1H and $^{13}C(CH_4)$ NMR results reveal that chemical shielding due to CH_4 molecule adsorption are also dependent upon the nanotube electronic structure, and radius. Due to the physisorption, NQR parameters of hydrogen atoms are also altered. The asymmetry parameter increases (by 0.0003-0.007 units).

REFERENCES

[1] N. Hamada, S.-I. Sawada, A. Oshiyama, Phys. Rev. Lett. 68 (1992) 1579.

[2] L. Lai, J. Lu, W. Song, M. Ni, L. Wang, G. Luo, J. Zhou, W.N. Mei, Z. Gao, D. Yu, J. Phys. Chem. C 112 (2008) 16417.

[3] A. Kuznetsova, J.T. Yates, J. Liu, R.E. Smalley, J. Chem. Phys. 112 (2000) 9590.

[4] A. Kuznetsova, J.T. Yates, V.V. Simonyan, J.K. Johnson, C.B. Huffman, R.E. Smalley, J. Chem. Phys. 115 (2001) 6691.

[5] O. Byl, P. Kondratyuk, S.T. Forth, S.A. FitzGerald, J.K. Chen, J.T. Johnson, J. Yates, J. Am. Chem. Soc. 125 (2003) 5889.

[6] A. Lubezky, L. Chechelnitsky, M. Folman, J. Chem. Soc., Faraday Trans. 92 (1996) 2269.

[7] M. Fastow, Y. Kozirovski, M. Folman, J. Heidberg, J. Phys. Chem. 96 (1992) 6126.

[8] A. Lubezky, L. Chechelnitsky, M. Folman, Surf. Sci. 454 (2000) 147.

[9] J.W.G. Wildoer, L.C. Venema, A.G. Rinzler, R.E. Smalley, C. Dekker, Nature 391 (1998) 59.

[10] A.G. Marinopoulos, L. Reining, A. Rubio, N. Vast, Appl. Phys. A: Mater. Sci. Process. 78 (2004) 1157.

[11] R.B. Weisman, S.M. Bachilo, D. Tsyboulski, Appl. Phys. A: Mater. Sci. Process 78 (2004) 1111.

[12] M.S. Dresselhaus, G. Dresselhaus, R. Saito, A. Jorio, Phys. Rep. 409 (2005) 47.
[13] N.A. Besley, J.J. Titman, M.D. Wright, J. Am. Chem. Soc. 127 (2005) 17948.
[14] D. Canet, Nuclear Magnetic Resonance: Concepts and Methods, Wiley, Chichester, 1996.
[15] G.K. Semin, T.A. Babushkina, G.G. Yakobson, Nuclear Quadrupole Resonance in Chemistry, Wiley, New York, 1975.
[16] N.A. Gershenfeld, I.L. Chuang, Science 275 (1997) 350.
[17] D.G. Gory, A.F. Fahmy, T.F. Havel, Proc. Natl. Acad. Sci. USA 94 (1997) 1634.
[18] J.A. Jones, Fort. Der Physik 48 (2000) 909.
[19] A.R. Kessel, V.L. Ermakov, JETP Lett. 70(1999) 61.
[20] A.K. Khitrin, B.M. Fung, J. Chem. Phys. 112 (2000) 6963.
[21] A.K. Khitrin, H. Song, B.M. Fung, Phys. Rev. A 63 (2001) 1.
[22] X.-P. Tang, A. Kleinhammes, H. Shimoda, L. Fleming, K.Y. Bennoune, S. Shina, C. Bower, O. Zhou, Y. Wu, Science 288 (2000) 492.
[23] S. Hayashi, F. Hoshi, T. Ishikura, M. Yumura, S. Ohshima, Carbon 41 (2003) 3047.
[24] H. Peng, L.B. Alemany, J.L. Margrave, V.N. Khabashesku, J. Am. Chem. Soc. 125 (2003) 15174.
[25] L.S. Cahill, Z. Yao, A. Adronov, J. Penner, K.R. Moonoosawmy, P. Kruse, G.R. Goward, J. Phys. Chem. B 108 (2004) 11412.
[26] X.-P. Tang, A. Kleinhammes, H. Shimoda, L. Fleming, K.Y. Bennoune, S. Sinha, C. Bower, O. Zhou, Y. Wu, Science 288 (2000) 492.
[27] C. Goze-Bac, S. Latil, P. Lauginie, V. Jourdain, J. Conard, L. Duclaux, A. Rubio, P. Bernier, Carbon 40 (2002) 1825.
[28] S. Hayashi, F. Hoshi, T. Ishikura, M. Yumura, S. Ohshima, Carbon 41 (2003) 3047.
[29] A. Kleinhammes, S.-H. Mao, X.-J. Yang, X.-P. Tang, H. Shimoda, J.P. Lu, O. Zhou, Y. Wu, Phys. Rev. B 68 (2003) 754181.
[30] M.J. Frisch, G.W. Trucks, H.B. Schlegel, G.E. Scuseria, M.A. Robb, J.R. Cheeseman, V.G. Zakrzewski, J.A. Montgomery, R.E. Stratmann, J.C. Burant, S. Dapprich, J.M. Millam, A.D. Daniels, K.N. Kudin, M.C. Strain, O. Farkas, J. Tomasi, V. Barone, M. Cossi, R. Cammi, B. Mennucci, C. Pomelli, C. Adamo, S. Clifford, J. Ochterski, G.A. Petersson, P.Y. Ayala, Q. Cui, K. Morokuma, D.K. Malick, A.D. Rabuck, K. Raghavachari, J.B. Foresman, J. Cioslowski, J.V. Ortiz, A.G. Baboul, B.B. Stefanov, G. Liu, P. Liashenko, A. Piskorz, I. Komaromi, R. Gomperts, R.L. Martin, D.J. Fox, T. Keith, M.A. Al-Laham, C.Y. Peng, A. Nanayakkara, C. Gonzalez, M. Challacombe, P.M.W. Gill, B. Johnson, W. Chen, M.W. Wong, J.L. Andres, C. Gonzalez, M. Head-Gordon, E.S. Replogle, J.A. Pople, Gaussian, Gaussian Inc., Pittsburgh, P B, 2003.
[31] S. Grimme, J. Comp. Chem. 27 (2006) 1787.
[32] J.T. Frey, D.J. Doren TubeGen 3.3; University of Delaware: Newark, DE, web interface, http://turin.nss.udel.edu/research/tubegenonline.html, 2005.
[33] F.A. Hamprecht, A. Cohen, D.J. Tozer, N.C. Handy, J. Chem. Phys. 109 (1998) 6264.
[34] E.A.C. Lucken, Nuclear Quadrupole Coupling Constants, Academic Press, London, 1992.
[35] P. Pyykkö, Mol. Phys. 99 (2001) 1617.
[36] G. Vidali, G. Ihm, H.Y. Kim, M.W. Cole, Surf. Sci. Rep. 12 (1991) 133.
[37] M.R. Johnson, S. Rols, P. Wass, M. Muris, M. Bienfait, P. Zeppenfeld, N. Dupont-Pavlovsky, Chem. Phys. 293 (2003) 217.
[38] S. Talapatra, V. Krugleviciute, A.D. Migone, Phys. Rev. Lett. 89 (2002) 2461061.
[39] B.K. Agrawal, S. Agrawal, S. Singh, R. Srivastava, J. Phys. Condens. Matter 18 (2006) 4649.
[40] L. Lai, J. Lu, W. Song, M. Ni, L. Wang, G. Luo, J. Zhou, W.N. Mei, Z. Gao, D. Yu, J. Phys. Chem. C 112 (2008) 16417.
[41] E. Zurek, J. Autschbach, J. Am. Chem. Soc. 126 (2004) 13079.
[42] E. Zurek, C.J. Pickard, B.J. Autschbach, J. Phys. Chem. C 112 (2008) 9267.